Journal of Southeast University (English Edition) Vol. 37, No. 4, pp. 401 - 407 Dec. 2021 ISSN 1003—7985

Evaluation of mechanical properties of cast steel nodes based on GTN damage model

Jiao Haihan[1,2] Yan Huadong[1,3] Jin Hui[1,2]

([1]Jiangsu Key Laboratory of Engineering Mechanics, Southeast University, Nanjing 211189, China)
([2]School of Civil Engineering, Southeast University, Nanjing 211189, China)
([3]Test and Measuring Academy of Norinco Group, Huayin 714200, China)

Abstract: Based on the Gurson-Tvergaard-Needleman (GTN) damage model considering the defect damage evolution, the influence of void defects caused by the casting process on cast steel nodes' mechanical properties was studied. Firstly, based on the GTN damage model, the model's parameter combination of G20Mn5N cast steel was given. Then, the mechanical properties of cast steel nodes were evaluated using the GTN damage model in ABAQUS software, and the influence of model parameters on the failure results was investigated. The results show that the cast steel node considering the GTN damage model fails under 1.93 times of the load. The bearing capacity is lower than that of the bilinear model, and the failure speed is faster. Changes in model parameters will cause a shift in the failure critical point. Meanwhile, the plastic strain index affects the void volume fractions, which shows different variation laws under uniaxial tensile and cyclic loads. Therefore, the GTN damage model establishes the relationship between the micro-defects and macro-mechanical properties of materials, which can better simulate the failure results of structures.

Key words: cast steel node; Gurson-Tvergaard-Needleman (GTN) damage model; bearing capacity; model parameters
DOI: 10.3969/j.issn.1003 - 7985.2021.04.009

Cast steel nodes are a kind of prefabricated integral casting node. They have flexible and various forms and a good mechanical performance and hence are an ideal form for complex structural nodes[1]. However, the number of cast steel's void defects is far more than that of hot-rolled steel because of different production processes[2]. The existence of defects destroys the material's continuity, leading to a decline in the structure's mechanical properties.

Received 2021-05-08, **Revised** 2021-09-29.
Biographies: Jiao Haihan (1997—), male, graduate; Jin Hui (corresponding author), female, doctor, professor, jinhui@seu.edu.cn.
Foundation items: The National Key Research and Development Program of China (No. 2017YFC0805100), the National Natural Science Foundation of China (No. 51578137), the Priority Academic Program Development of Jiangsu Higher Education Institutions, the Open Research Fund Program of Jiangsu Key Laboratory of Engineering Mechanics.
Citation: Jiao Haihan, Yan Huadong, Jin Hui. Evaluation of mechanical properties of cast steel nodes based on GTN damage model[J]. Journal of Southeast University (English Edition), 2021, 37(4): 401 - 407. DOI: 10.3969/j.issn.1003 - 7985.2021.04.009.

Metal is a ductile material, whose failure is often related to the nucleation, growth, and coalescence of voids caused by a load until macroscopic cracks are formed[3]. Therefore, it is necessary to examine the changes of microvoids and their effects on the macro-mechanics of materials to truly reflect the damage evolution process. However, the traditional industrial flaw detection method has low accuracy, making it difficult to determine the distribution and size of micro-defects inside the casting. Moreover, the original bilinear model does not consider internal material damages, causing insufficient assessment of the structural safety and reliability.

In fracture mechanics, current constitutive material models can be divided into two types: Macroscopic models, such as the Lemaitre model, do not consider the micromechanisms of ductile damage[3-4]. Gurson[5] coupled the evolution of voids with the equivalent plastic strain of a material based on volume cell models and deduced a relatively complete microscopic damage model. Subsequently, Tvergaard[6] and Needleman et al.[7] modified the model and formed the Gurson-Tvergaard-Needleman (GTN) damage model, which is widely used in the research of metal properties. This model uses the yield function to describe the yield behavior of materials and the void volume fraction to define the failure of materials, which can accurately describe the failure results of metal materials compared with the bilinear model[8].

Since the proposal of the GTN damage model, many scholars have applied it to simulate the damage evolution process of metals. Xu et al.[9] simulated the tensile behavior of corroded reinforcing bars in concrete under a carbonized environment. Liu et al.[10] simulated the effect of MnS inclusions on the initiation and propagation of cracks in as-cast 304 stainless steel at high temperatures. Steglich et al.[11] studied the interaction between the plastic anisotropy and void growth of aluminum alloy 2198. The above instances fully indicate that the GTN damage model promotes the development of micro-damage mechanics and establishes a good connection between experimental verifications and the finite element method (FEM), and its application has become increasingly widespread[12].

In this study, the bearing capacity of cast steel nodes

was calculated based on the bilinear model and GTN damage model. The relationship between the model parameters and the failure results of cast steel nodes under different loads was also examined.

1 GTN Damage Model and Its Parameters

1.1 GTN damage model

The yield function of the GTN damage model can be expressed as follows:

$$\Phi = \left(\frac{\sigma_{eq}}{\sigma_y}\right)^2 + 2q_1 f^* \cosh\left(-\frac{3q_2\sigma_m}{2\sigma_y}\right) - (1 + q_3 f^{*2}) = 0 \tag{1}$$

where σ_{eq} is the effective von Mises stress; σ_y is the initial yield stress of the matrix material; σ_m is the hydrostatic stress; q_1, q_2, and $q_3 = q_1^2$ are the correction parameters.

The damage variable f^* is a function of the total void volume fraction f, which is expressed as

$$f^*(f) = \begin{cases} f & f_0 \leqslant f \leqslant f_c \\ f_c + \dfrac{f_u^* - f_c}{f_f - f_c}(f - f_c) & f_c < f \leqslant f_f \\ f_u^* = \dfrac{1}{q_1} & f > f_f \end{cases} \tag{2}$$

where f_0 is the initial void volume fraction; f_c is the critical void volume fraction; f_f is the void volume fraction at the fracture; f_u^* is the ultimate value of the damage parameter.

The yield surface of the GTN damage model connects the yield with the damage of the material, so the yield surface will gradually shrink with the increase in f^*, reflecting the continuous deterioration of materials due to damage evolution, as shown in Fig. 1. When $f^* = 0$, Eq. (1) degenerates into a von Mises yield function.

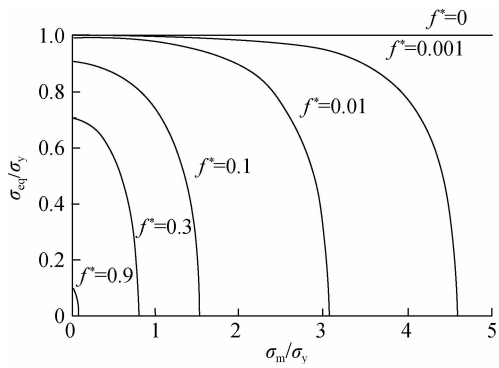

Fig. 1 Yield surface of the GTN damage model

The total void volume fraction f in the GTN damage model includes the initial void volume fraction f_0, growing void volume fraction f_{gr}, and nucleated void volume fraction f_{nu}:

$$f = f_0 + f_{gr} + f_{nu} \tag{3a}$$

The increment expression is

$$\mathrm{d}f = \mathrm{d}f_{gr} + \mathrm{d}f_{nu} \tag{3b}$$

Due to the incompressibility of the matrix material, the growth of the initial voids depends on the plastic strain[13]:

$$\mathrm{d}f_{gr} = (1 - f)\,\mathrm{d}\varepsilon_p : I \tag{4}$$

where ε_p is the plastic strain and I is the second-order unit tensor.

Generally, nucleation will only occur when the stress exceeds the critical value, and the number of nucleation increases with the strain's increase[14]:

$$\mathrm{d}f_{nu} = \frac{f_N}{S_N\sqrt{2\pi}}\exp\left[-\frac{1}{2}\left(\frac{\bar{\varepsilon}_p - \varepsilon_N}{S_N}\right)^2\right]\mathrm{d}\bar{\varepsilon}_p \tag{5}$$

where $\bar{\varepsilon}_p$ is the equivalent plastic strain; f_N is the volume fraction of void nucleating particles; ε_N is the mean nucleation strain; S_N is the corresponding standard deviation.

Eqs. (1) to (5) constitute the GTN damage model, which can simulate the entire process of void nucleation, growth, coalescence, and fracture. In this model, Eqs. (3) to (5) describe the nucleation and growth of voids, and Eqs. (1) to (2) determine the influence of voids' coalescence and fracture on the bearing capacity.

1.2 Parameters in the GTN damage model

The GTN damage model has nine parameters, which can be divided into three groups. The first group is the correction parameters, including q_1, q_2, and q_3; the second is the void volume fractions, including f_0, f_c, and f_f; and the third is the nucleation parameters, including f_N, ε_N, and S_N. To construct the GTN damage model, it is necessary to calibrate the optimal combination of parameters. At present, the common methods to calibrate the parameter values in the GTN damage model are metallographic analysis, cell element method, and finite element reverse method[12]. However, even with the proposal of the GTN damage model, it was not easy to obtain all the parameters through experiments because of their numerous material parameters. Therefore, researchers studied on the model parameters' calibration of different materials and achieved some results[4, 10, 15–20], which provide a reliable basis for applying the model.

Yan et al.[21–23] calibrated the model parameters of G20Mn5N cast steel using the finite element reverse method combining the three-dimensional X-ray microtomography technique and numerical simulation. The results in Tab. 1 show that the numerical simulation results are in good agreement with the experimental results.

Tab. 1 Optimal combination of the GTN damage model for G20Mn5N cast steel

q_1	q_2	q_3	$f_0/10^{-3}$	f_c	$f_f/10^{-2}$	f_N	ε_N	S_N
1.5	1.0	2.25	2.7	0.03	4.5	0.01	0.25	0.05

2 Evaluation of Cast Steel Node's Bearing Capacity

2.1 Material properties

The cast steel node selected in this study has four intersecting tubes, located in a large-span steel structure. The overall schematic diagram of the node and the number of each tube are shown in Fig. 2. The material of the cast steel node is G20Mn5N cast steel, and its chemical composition and basic mechanical properties are shown in Tabs. 2 and 3.

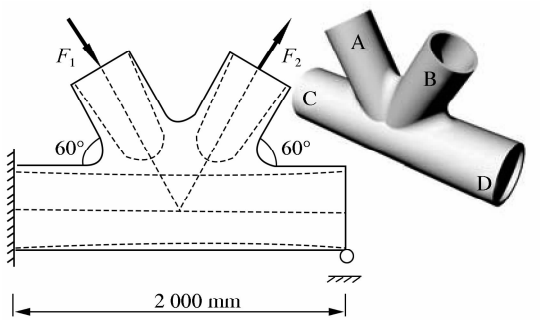

Fig. 2 Overall schematic diagram of the cast steel node

Tab. 2 Chemical composition of the G20Mn5N cast steel %

Item	Regulation	Test
w(C)	0.17 to 0.23	0.196 0
w(Si)	≤0.60	0.419 0
w(Mn)	1.00 to 1.60	1.530 0
w(S)	≤0.020	0.017 0
w(P)	≤0.020	0.011 6
w(Ni)	≤0.80	0.268 0

Tab. 3 Mechanical properties of the G20Mn5N cast steel

Item	Elastic modulus/GPa	Yield strength/MPa	Ultimate strength/MPa	Elongation/%
Regulation	206	300	480 to 620	≥20
Test	230	320	483	31.9

2.2 Establishment of the cast steel node model

The FEM software ABAQUS was used to model and calculate the cast steel node with C3D10m solid elements. A fixed constraint is imposed on the main tube port C. A displacement constraint in the X and Y directions is imposed on the main tube port D. According to the requirements of JGJ/T 395—2017[24], the main part of the cast steel node should be in an elastic stage under complex stress. Meanwhile, the local stress concentration area is allowed to transit to the plastic stage. Therefore, a 1 161 284N compressive load is applied to branch tube port A, and a 2 237 085N tensile load is applied to branch tube port B.

There are stress concentration areas at the branch tube ports A and B, so mesh encryption is performed in these areas. Tab. 4 and Fig. 3 show different mesh densities cases. Fig. 4 shows the stress and displacement calculation results of branch tube port B by different cases. The model's von Mises stress and resultant displacement results stabilize when the branch tube port's mesh density reaches 9 mm, so this mesh density is selected for calculation.

Tab. 4 Different mesh density cases mm^2

Case	Mesh encryption area	Mesh transition area	Mesh sparsity area
1	15	15	15
2	12	13	15
3	9	12	15
4	7	10	15
5	5	9	15

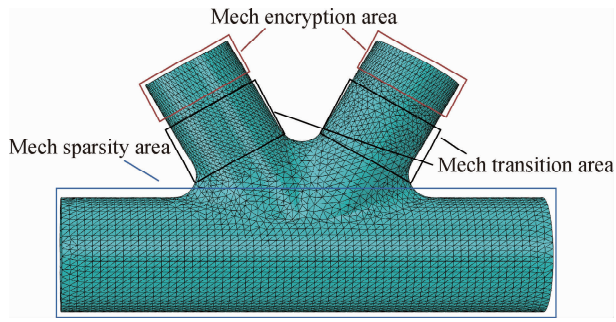

Fig. 3 Mesh density model of the cast steel node

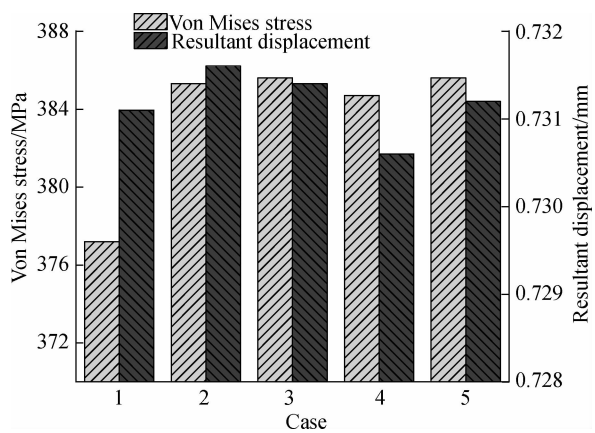

Fig. 4 Von Mises stress and resultant displacement results by different mesh densities

2.3 Service limit state

Figs. 5 and 6 show the Von Mises stress and the equivalent plastic strain contour of the cast steel node calculated by the bilinear model and GTN damage model under the design load. Branch tube port B yields based on the two constitutive models, but the yielding area is small and most areas are still in the elastic stage.

The maximum Von Mises stress values of cast steel nodes calculated based on the two constitutive models are 364 and 386 MPa. The difference between the two values is minute, and the value based on the GTN damage model is slightly large. Whether the damage is considered or

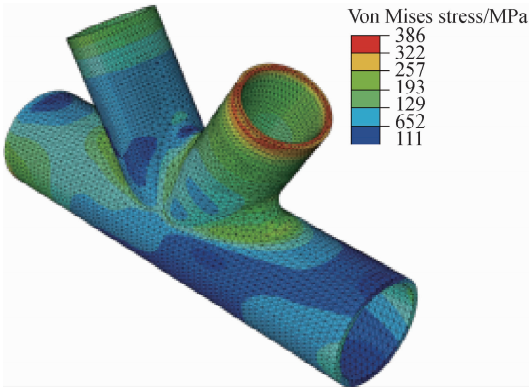

(a)

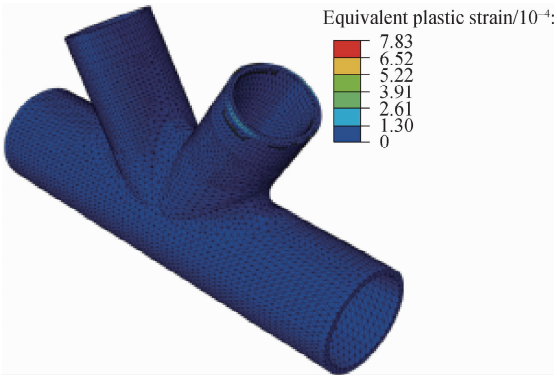

(b)

Fig. 5 FEM results based on the GTN damage model. (a) Von Mises stress contour; (b) Equivalent plastic strain contour

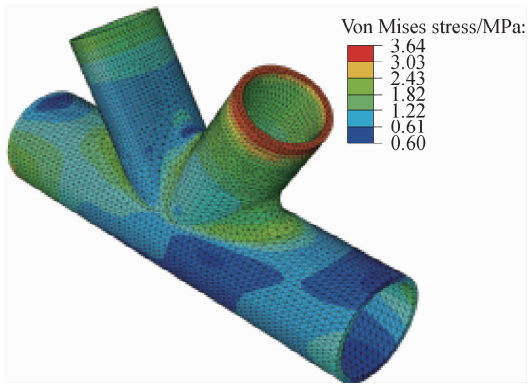

(a)

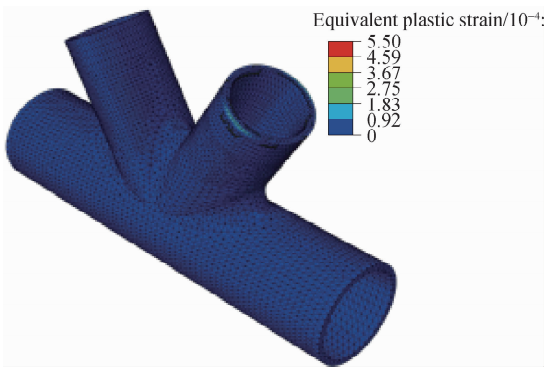

(b)

Fig. 6 FEM results based on the bilinear model. (a) Von Mises stress contour; (b) Equivalent plastic strain contour

not has little effect on the service limit state of cast steel nodes. The reason is that the main areas of cast steel nodes do not transit to a yielding stage under the design load, and the damage in the nodes has not yet evolved.

2.4 Ultimate limit state

The ultimate limit state of the cast steel node mainly refers to the maximum axial force when the node is damaged due to excessive local deformation under a load[25]. According to JGJ/T 395—2017[24], the extreme point of the load-displacement curve calculated by the FEM should be taken as the ultimate limit capacity.

Fig. 7 shows the load-displacement curves of the branch tube ports A and B calculated by the two constitutive models. Whether the bilinear model or GTN damage model is adopted, branch tube port A yields before branch tube port B, but the relative displacement in the ultimate limit state for branch tube port B is greater than that of branch tube port A.

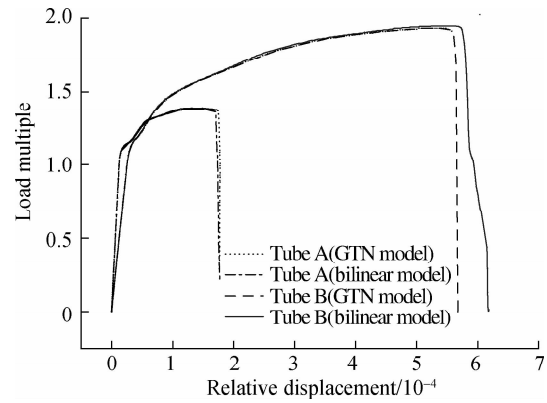

Fig. 7 Load multiple-relative displacement curve of branch tube ports A and B

The load-displacement curves obtained by the two constitutive models have good consistency in the elastic, yielding, and coinciding in the strengthening stage, but there are differences in the degradation stage. The load-displacement curve calculated by the GTN damage model fails earlier, and the strength decreases faster. The ultimate bearing capacity based on the bilinear model and GTN damage model is 1.95 and 1.93 times of the load, respectively, which meets the requirements of JGJ/T 395—2017 that the ultimate limit capacity should be 1.5 times greater than the design load.

Based on this analysis, the damage evolution behavior of materials has a specific impact on the ultimate limit state of the cast steel node. After considering the material performance degradation caused by damage, the failure process of components after reaching the ultimate limit capacity is rapid. Although the stress level of cast steel nodes in the service limit state is in the elastic stage, it is likely to transit the plastic stage under ultimate loads, such as seismic action. The GTN damage model can ef-

fectively predict the failure results of cast steel nodes in the ultimate limit state.

3 Model Parameters in the GTN Damage Model

3.1 Effect of model parameters on the load-displacement curves

After evaluating the bearing capacity of the cast steel node, the effects of the model parameters (f_c, f_f, f_N, and ε_N) on the load-displacement curves of the cast steel node were studied.

Fig. 8 shows that f_c does not affect the curve's trend, but for the same void nucleation and growth rate, the larger f_c is, the longer the time needed for the void to coalesce. Therefore, the critical failure point will be delayed.

The influence of f_f on the curve is similar to f_c. When the test conditions and other model parameters are identical, the larger f_f is, the longer the voids needed nucleate and grow to f_f, and the critical failure point will move backward.

By increasing f_N, the larger the void volume fraction is due to the micro-defects in the material, the faster the critical failure point will be reached, leading to a short fracture displacement.

df_{nu} is an approximately normal distribution concerning an equivalent plastic strain, so the strain at the maximum point of the void nucleation velocity is ε_N. The larger the ε_N is, the smaller the void nucleation velocity is, and the higher the bearing capacity of cast steel nodes is.

3.2 Evolution of the void volume fraction under a load

In this section, we examine the evolution of the void volume fraction (f, f_{gr}, and f_{nu}) and plastic strain index (PEMAG and PEEQ) by the GTN damage model. The uniaxial tensile load and cyclic load applied to the cast steel node are shown in Figs. 9 and 10. The evolution of the void volume fraction and plastic strain index at branch tube port B are shown in Figs. 11 and 12.

Fig. 11 shows the evolution of the variables under auniaxial tensile load. When the materials transit to the yielding stage under the load, f_{gr} and f_{nu} rapidly increase after the PEEQ (equivalent plastic strain) accumulates to a certain extent, and f_{nu} increases faster. f and the PEMAG (plastic strain magnitude) have similar variations, indicating that the GTN damage model effectively couples the damage parameters and the plastic strain of the matrix material. It also explains why the bilinear and GTN damage models' load-displacement curves differ after the yielding stage.

Fig. 12 shows the evolution of these variables under a cyclic load. f rises in steps during the load process, and the growth rate becomes increasingly faster. Eq. (4) shows that f_{gr} is related to PEMAG. PEMAG is positive

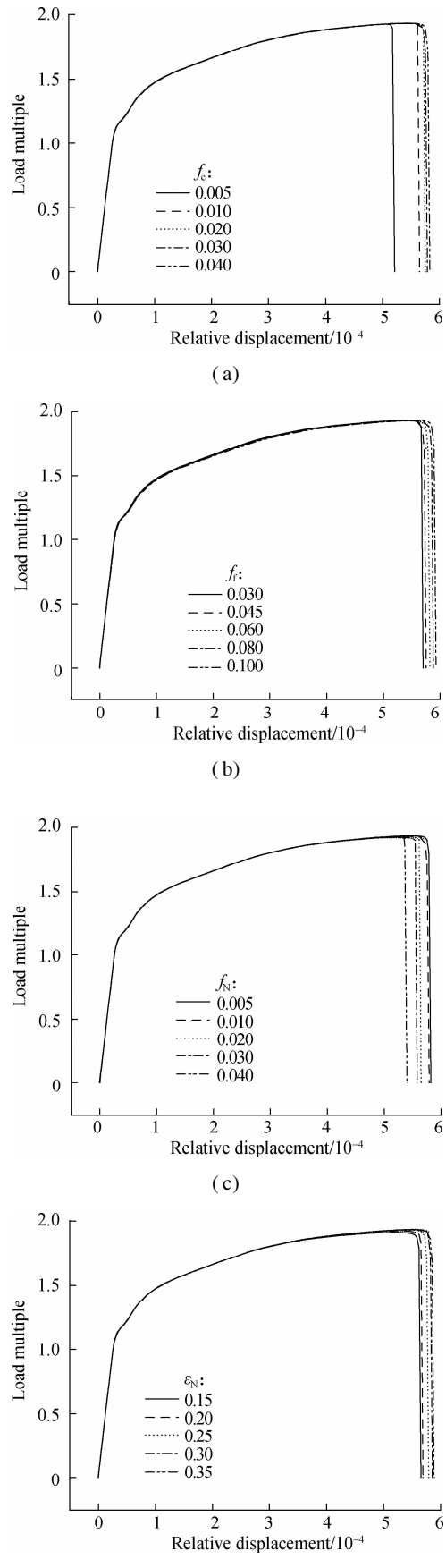

Fig. 8 Effects of nucleation parameters on the load multiple-relative displacement curves. (a) f_c; (b) f_f; (c) f_N; (d) ε_N

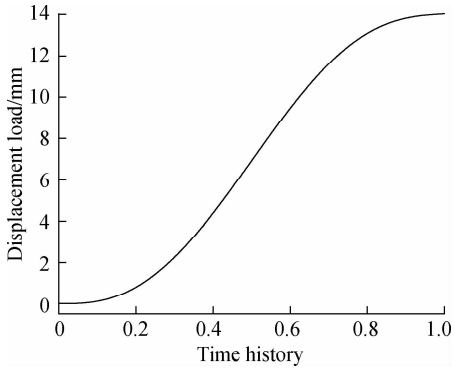

Fig. 9 Uniaxial tensile load

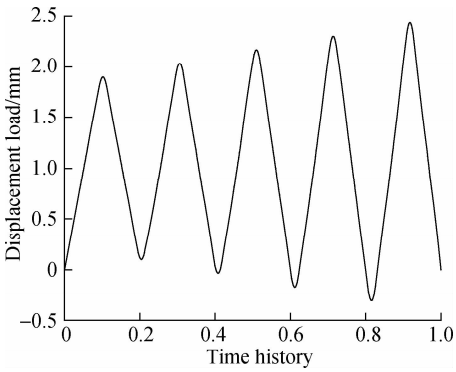

Fig. 10 Cycle load

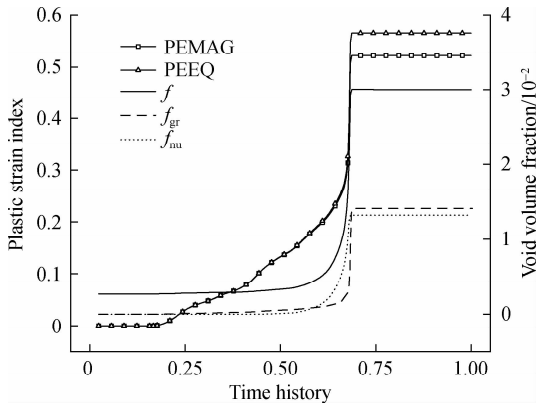

Fig. 11 Evolution of the void volume fraction and plastic strain index with a uniaxial tensile load

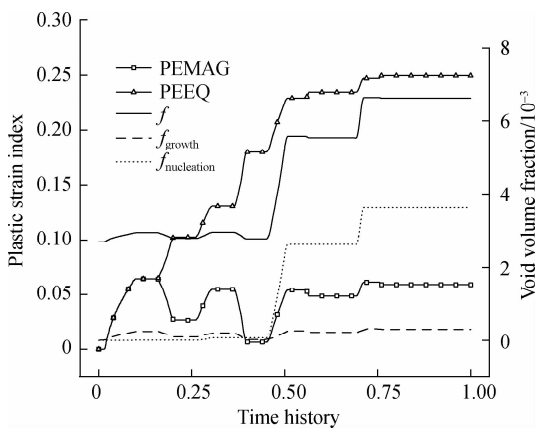

Fig. 12 Evolution of the void volume fraction and plastic strain index with a cycle load

during tension and negative during compression. Therefore, f_{gr} changes positively and negatively with the cyclic load, and its horizontal stage corresponds to the unloading stage. Eq. (5) shows that f_{nu} is related to the PEEQ. The PEEQ increases during the loading stage and remains unchanged during the unloading stage, so f_{nu} rises in steps during the loading process.

4 Conclusions

1) Based on the bilinear model and GTN damage model, the bearing capacity of the cast steel node was evaluated. The results show that there is a specific influence on the ultimate limit state. The cast steel node has an earlier failure time and faster failure speed considering the GTN damage model.

2) The influence of each model parameter on the failure critical point of the cast steel node was compared and analyzed. The results show that as f_N increases, the critical failure point moves forward; as f_c, f_f, and ε_N increase, the critical failure point moves backward.

3) The evolution of the void volume fraction and plastic strain index is similar under the uniaxial tensile load. However, under the cyclic load, f_{gr} and f_{nu} are respectively affected by the PEMAG and PEEQ, which show different evolution laws.

References

[1] Yin Y, Li S, Han Q H, et al. Material parameters in void growth model for G20Mn5QT cast steel at low temperatures[J]. *Construction and Building Materials*, 2020, **243**: 1 − 15. DOI: 10.1016/j.conbuildmat.2020.118123.

[2] Blair M, Monroe R, Beckermann C, et al. Predicting the occurrence and effects of defects in castings[J]. *The Journal of The Minerals*, 2005, **57**(5): 29 − 34. DOI: 10.1007/s11837-005 − 0092-3.

[3] Zhao C F, Li Z X. Influence of geometrical features of meso-defects on damage evolution of metal structure[J]. *Applied Mechanics and Materials*, 2015, **723**: 21 − 25. DOI: 10.4028/www.scientific.net/AMM.723.21.

[4] Springmann M, Kuna M. Identification of material parameters of the Gurson-Tvergaard-Needleman model by combined experimental and numerical techniques[J]. *Computational Materials Science*, 2005, **32**(3/4): 544 − 552. DOI: 10.1016/j.commatsci.2004.09.010.

[5] Gurson A L. Porous rigid-plastic materials containing rigid inclusions-yield function, plastic potential, and void nucleation[J]. *Physical Metallurgy of Fracture*, 1978 (5): 357 − 364. DOI: 10.1016/B978-0 − 08-022138-0.50058-7.

[6] Tvergaard V. Influence of voids on shear band instabilities under plane-strain conditions[J]. *International Journal of Fracture*, 1981, **17**(4): 389 − 407. DOI: 10.1007/BF00036191.

[7] Needleman A, Tvergaard V. An analysis of ductile rupture in notched bars[J]. *Journal of the Mechanics and Physics of Solids*, 1984, **32**(6): 461 − 490. DOI: 10.1016/0022-5096(84)90031-0.

[8] Roux E, Bernacki M, Bouchard P O. A level-set and anisotropic adaptive remeshing strategy for the modeling of

void growth under large plastic strain[J]. *Computational Materials Science*, 2013, **68**: 32 - 46. DOI: 10.1016/j.commatsci.2012.10.004.

[9] Xu Y D, Qian C X. Application of Gurson-Tvergaard-Needleman constitutive model to the tensile behavior of reinforcing bars with corrosion pits[J]. *Plos One*, 2017, **8**(1): 1 - 7. DOI: 10.1371/journal.pone.0054368.

[10] Liu X G, Wang C, Deng Q F, et al. High-temperature fracture behavior of MnS inclusions based on GTN model [J]. *Journal of Iron and Steel Research International*, 2019, **26**: 941 - 952. DOI: 10.1007/s42243-018 - 0202-4.

[11] Steglich D, Wafai H, Besson J. Interaction between anisotropic plastic deformation and damage evolution in Al 2198 sheet metal[J]. *Engineering Fracture Mechanics*, 2010, **77**(17): 3501 - 3518. DOI: 10.1016/j.engfracmech.2010.08.021.

[12] Li G, Cui S S. A review on theory and application of plastic meso-damage mechanics[J]. *Theoretical and Applied Fracture Mechanics*, 2020, **109**: 1 - 12. DOI: 10.1016/j.tafmec.2020.102686.

[13] Zhang Z L, Thaulow C, Ødegård J. A complete Gurson model approach for ductile fracture[J]. *Engineering Fracture Mechanics*, 2000, **67**(2): 155 - 168. DOI: 10.1016/S0013-7944(00)00055-2.

[14] Chu C C, Needleman A. Void Nucleation effects in biaxially stretched sheets[J]. *Journal of Engineering Materials and Technology*, 1980, **102**(3): 249 - 256. DOI: 10.1115/1.3224807.

[15] Acharyya S, Dhar S. A complete GTN model for prediction of ductile failure of pipe[J]. *Journal of Materials Science*, 2008, **43**(6): 1897 - 1909. DOI: 10.1007/s10853-007 - 2369-0.

[16] Zhou J, Gao X, Sobotka J C, et al. On the extension of the Gurson-type porous plasticity models for prediction of ductile fracture under shear-dominated conditions[J]. *International Journal of Solids and Structures*, 2014, **51**(18): 3273 - 3291. DOI: 10.1016/j.ijsolstr.2014.05.028.

[17] Kami A, Dariani B M, Vanini A S, et al. Numerical determination of the forming limit curves of anisotropic sheet metals using GTN damage model[J]. *Journal of Materials Processing Technology*, 2014, **216**: 472 - 483. DOI: 10.1016/j.jmatprotec.2014.10.017.

[18] Zhao P J, Chen Z H, Dong C F. Experimental and numerical analysis of micromechanical damage for DP600 steel in fine-blanking process[J]. *Journal of Materials Processing Tech*, 2016, **236**: 16 - 25. DOI: 10.1016/j.jmatprotec.2016.05.002.

[19] Jiang W, Li Y Z, Su J. Modified GTN model for a broad range of stress states and application to ductile fracture [J]. *European Journal of Mechanics A/solids*, 2016, **57**: 132 - 148. DOI: 10.1016/j.euromechsol.2015.12.009.

[20] Gholipour H, Biglari F R, Nikbin K. Experimental and numerical investigation of ductile fracture using GTN damage model on in-situ tensile tests[J]. *International Journal of Mechanical Sciences*, 2019, **164**: 1 - 15. DOI: 10.1016/j.ijmecsci.2019.105170.

[21] Yan H D, Jin H, Yao R G. Prediction of the damage and fracture of cast steel containing pores[J]. *International Journal of Damage Mechanics*, 2020, **29**(1): 1 - 18. DOI: 10.1177/1056789519872000.

[22] Yan H D, Tang Q, Jin H. Damage evolution analysis on cast steel joints with porosity defects[J]. *Journal of Southeast University* (*Natural Science Edition*), 2019, **49**(5): 904 - 910. DOI: 10.3969/j.issn.1001-0505.2019.05.013. (in Chinese)

[23] Yan H D, Jin H. Damage evolution analysis of cast steel GS-20Mn5V based on modified GTN model[J]. *Journal of Southeast University*(*English Edition*), 2018, **34**(3): 364 - 370.

[24] Ministry of Housing and Urban-rural Development of the People's Republic of China. Technical specification for cast steel structure: JGJ/T 395—2017[S]. Beijing: China Construction Industry Press, 2017. (in Chinese)

[25] Luo L S, Wen H G, Duan X N. Research on bearing capacity of circular steel tubular KX-joint[J]. *Steel Structure*, 2018, **33**(2): 56 - 59, 109. (in Chinese)

基于 GTN 损伤模型的铸钢节点力学性能评估

焦海涵[1,2]　闫华东[1,3]　靳　慧[1,2]

([1] 东南大学江苏省工程力学分析重点实验室,南京 211189)

([2] 东南大学土木工程学院,南京 211189)

([3] 中国兵器工业试验测试研究院,华阴 714200)

摘要:基于考虑缺陷损伤演化过程的 GTN 损伤模型,研究了铸造工艺引起的孔洞缺陷对铸钢节点力学性能的影响. 首先,基于 GTN 损伤模型推导出 G20Mn5N 铸钢 GTN 模型的最佳参数组合. 然后,在 ABAQUS 软件中利用 GTN 损伤模型对铸钢节点的力学性能进行评估,并研究了模型参数对铸钢节点破坏过程的影响. 结果表明,考虑 GTN 损伤模型的铸钢节点在 1.93 倍的载荷下发生破坏,承载能力低于二折线模型,且破坏速度更快. 模型参数的改变会导致临界失效点移动. 孔隙体积分数的变化规律受塑性应变指数的影响,并在单向拉伸载荷和循环载荷下呈现出不同的变化规律. GTN 损伤模型建立了材料微观缺陷与宏观力学性能之间的关系,能够较好地模拟结构的破坏过程.

关键词:铸钢节点;GTN 损伤模型;承载能力;模型参数

中图分类号:TU512. 9